Structural changes in ferroelectric phase transitions of vinylidene fluoride–tetrafluoroethylene copolymers: 2. Normal-modes analysis of the infra-red and Raman spectra at room temperature

Kohji Tashiro*, Hiroyoshi Kaito and Masamichi Kobayashi
Department of Macromolecular Science, Faculty of Science, Osaka University, Toyonaka, Osaka 560, Japan
(Received 20 July 1991; accepted 29 August 1991)

Normal-modes calculation was made for a series of model polymer chains of vinylidene fluoride–tetrafluoroethylene (VDF–TFE) copolymers so as to interpret the systematic variation in the i.r. and Raman spectra. The model chains are alternating copolymers of $[-(VDF)_m(TFE)_n-]$ with $m/n = \infty/0$, 8/2, 5/5, 2/8 and $0/\infty$. Utilizing the normal-modes frequencies and the corresponding eigenvectors calculated for these model chains, the frequency–phase difference dispersion curves and the density of state (or the frequency distribution function) were constructed. Based on these results, the assignments of the intrinsic bands of the VDF sequence, TFE sequence and VDF–TFE boundary were made and the changes in the i.r. and Raman spectra observed at room temperature were interpreted.

(Keywords: vinylidene fluoride–tetrafluoroethylene copolymers; i.r. spectra; Raman spectra; normal-modes calculation; frequency–distribution curve)

INTRODUCTION

In our preceding paper[1] we investigated the structure and phase transition behaviour of vinylidene fluoride–tetrafluoroethylene (VDF–TFE) copolymers using X-ray diffraction and i.r. and Raman spectroscopy. As in the vinylidene fluoride–trifluoroethylene copolymers[2–6], the vibrational spectral data have been found to play an important role in clarifying the structural changes in the phase transition[1]. In particular the assignment of the intrinsic bands of the VDF sequence, the TFE sequence and the VDF–TFE boundary region enabled us to study the behaviour of these different regions of the chains. In order to confirm the band assignments and to clarify the nature of the bands, normal-mode calculations were carried out and the spectra were analysed in detail. In the present paper the i.r. and Raman spectra measured for the ferroelectric phase are interpreted by employing model polymer chains having structures similar to VDF–TFE copolymers.

PROCEDURE OF NORMAL-MODES CALCULATION

According to n.m.r., VDF–TFE copolymers are random copolymers with the VDF and TFE monomeric units distributed in a statistical fashion along the polymer chain[7]. One of the aims of this paper is to clarify the systematic change in the vibrational frequencies of the bands characteristic of the VDF and TFE segments which is caused by a variation in the segmental lengths. In order to perform the normal-modes calculation without any loss of essential structural features of the copolymers, the polymer chains are modelled as alternately repeating VDF and TFE segments of definite lengths as shown below:

$$-[-(CH_2CF_2)_m-(CF_2CF_2)_n]-$$

	m	n
PVDF	∞	0
VDF 80%	8	2
VDF 50%	5	5
VDF 20%	2	8
PTFE	0	∞

The molecular chains are assumed to take a planar zigzag conformation: this is reasonable judging from the X-ray diffraction results described in our previous paper[1]. The PTFE chain should originally have a helical conformation[8–10] but is assumed to take a zigzag form in this discussion[1]. This may also be reasonable, because the short TFE segments included in the copolymer chain are considered to take the zigzag form as discussed in detail in our preceding paper[1]. The bond lengths and bond angles are taken from references 11–13, where normal-mode analyses were carried out for PVDF forms I, II and III: C–C = 1.54 Å, C–F = 1.34 Å and C–H = 1.09 Å and ∠CCC, ∠HCH, ∠FCF, etc.,

*To whom correspondence should be addressed

0032-3861/92/142929-05

Table 1 Force constants used in the normal-modes calculation of the VDF–TFE copolymer models

No.	Force constants[a]	Coordinates involved	Common atoms	Values
1	K_d	CH		4.901
2	H_γ	CCH		0.627
3	H_δ	CHH		0.451
4	F_{Rd}	CC, CH	C	0.000
5	$F_{R\gamma}$	CC, CCH	C	0.206
6	F_d	CH, CH	C	0.058
7	F_γ	CCH, CCH	C	0.105
8	$F_{\gamma'}$	CCH, CCH	CH	0.074
9	$f_{\omega\gamma}(gauche)$	CCH, CCH(g)	CC	0.138
10	K_l	CF		6.549
11	H_ϕ	CCF		1.387
12	H_ζ	CFF		1.506
13	F_{Rl}	CC, CF	C	−0.091
14	$F_{R\phi}$	CC, CCF	CC	0.548
15	F_{ll}	CF, CF	C	0.151
16	$F_{l\zeta}$	CF, CFF	C	1.297
17	$F_{l\phi}$	CF, CCF	CF	1.058
18	$F_{\phi'}$	CCF, CCF	CF	0.234
19	F_ϕ	CCF, CCF	CC	0.176
20	$f_{\omega\phi}(gauche)$	CCC, CCF(g)	CC	−0.083
21	$f_\phi(trans)$	CCF, CCF(t)	CC	0.095
22	$f_\phi(gauche)$	CCF, CCF(g)	CC	−0.054
23	$f_\gamma(trans)$	CCH, CCF(t)	CC	0.063
24	$f_\gamma(gauche)$	CCH, CCF(g)	CC	0.055
25	$F_{d\gamma}$	CH, CCH	CH	0.041
26	$F_{d\delta}$	CH, CHH	CH	−0.132
27	K_R	CC		4.414
28	H_ω	CCC		1.199
29	F_R	CC, CC	C	0.148
30	$F_{R\omega}$	CC, CCC	CC	0.273
31	$F_\omega(trans)$	CCC, CCC(t)	CC	−0.036
32	T	CCCC		0.050

[a]Units of the force constants: stretching, mdyn Å^{-1}; stretch-bending, mdyn rad^{-1}; bending, mdyn Å rad^{-2}

$=109.5°$. In the calculation of the normal-mode frequencies, the GF matrix method was employed with the cyclic boundary conditions taken into consideration[10]. The intramolecular force constants were of valence force field type. The numerical values of the force constants are listed in *Table 1*[11–13].

RESULTS AND DISCUSSION

Figures 1 and *2* show the polarized i.r. and Raman spectra of a series of VDF–TFE copolymers measured at room temperature. By investigating the systematic change in the relative intensity of the bands, we can distinguish the intrinsic bands of the VDF and TFE sequences. For example, in *Figure 1*, the bands in the 1400–1450 cm^{-1} region increase in intensity in parallel with an increase in VDF content and disappear in the spectra of PTFE and thus they should be assigned to the modes intrinsic to the VDF segment. Similarly the bands at 600–650 cm^{-1} are from TFE segments. In *Figure 2*, the Raman bands can be classified in the same way: the bands at ~1430 and 1280 cm^{-1} are from VDF sequences, while the bands at ~1380 and 380 cm^{-1} are from TFE segments. The bands in the 800–900 cm^{-1} region, however, behave in a somewhat peculiar fashion different from the bands in the other frequency regions. Hence, the following discussion will concentrate mainly on the 800–900 cm^{-1} region.

Figure 3 shows the vibrational frequencies of the symmetric CF_2 stretching modes calculated for the VDF 50% model, where the length and direction of the vertical lines represent the vibrational potential energy distribution and the phase relation (δ) between neighbouring monomeric units. Two kinds of vibrational modes can be extracted in this region: one is the mode with the phonon wave extending over the VDF segment (856, 838, 836 and 835 cm^{-1}); the other type is the mode in which the phonon is located at the boundary between the VDF and TFE segments (829 and 826 cm^{-1}). The wavenumbers calculated for all the model copolymers are summarized in *Figure 4a*. The wavenumbers of the symmetric CF_2 stretching modes are not so dispersed but are concentrated in a comparatively narrow frequency region. However the number of modes, or the

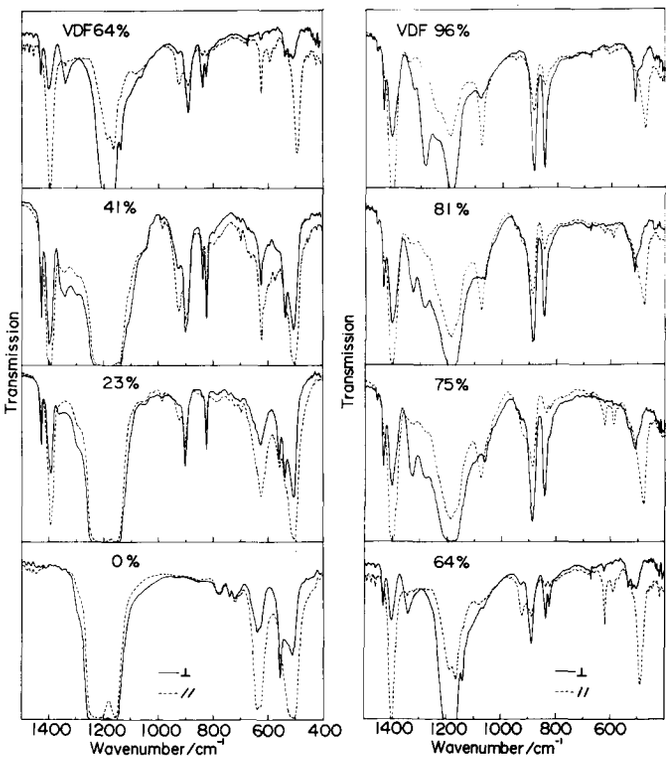

Figure 1 Polarized i.r. spectra of a series of oriented VDF–TFE copolymers taken at room temperature. Electric vector of the incident beam (——) perpendicular and (– – –) parallel to the orientation axis

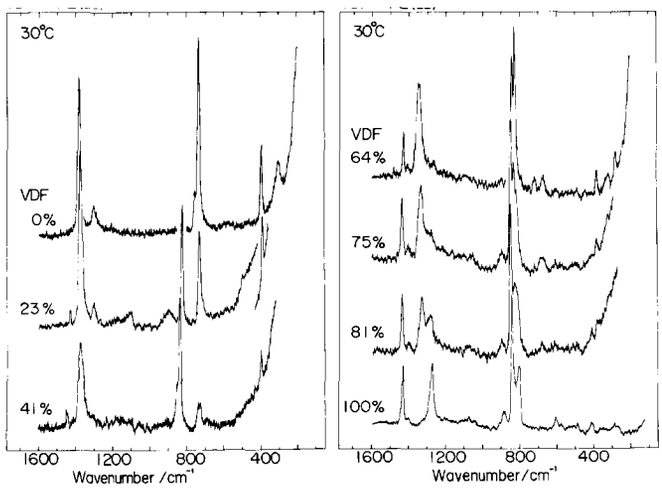

Figure 2 Polarized Raman spectra [(zz) component] of a series of uniaxially oriented VDF–TFE copolymers taken at room temperature

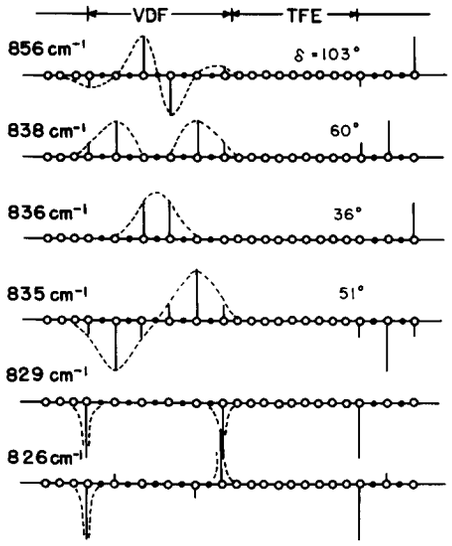

Figure 3 Examples of the calculated normal-mode frequencies and potential energy distribution (vertical lines) for the CF_2 oscillators representing the symmetric stretching mode (○). The solid circles represent CH_2 groups

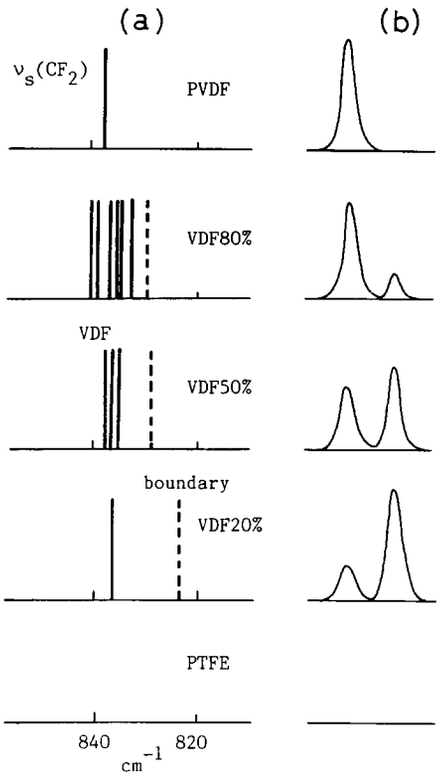

Figure 4 (a) Distribution of normal-mode frequencies of the CF_2 symmetric stretching modes calculated for the VDF–TFE copolymer models. (b) Schematic illustration of the predicted spectral change in the corresponding frequency region

vibrational density, gradually decreases with increasing TFE comonomer. On the other hand, the mode localized in the VDF–TFE boundary is located at an almost constant frequency position ($\sim 830\ cm^{-1}$). Therefore we can expect an interchange of the relative intensity between these two modes depending on the TFE content, as illustrated in *Figure 4b*. Although the absorption intensity should be expressed as a product of the so-called frequency distribution function and the transition dipole moments[14], the change in the vibrational mode density corresponds qualitatively to the actually observed spectral change as reproduced in *Figures 5* and *6*, where the decrease in the $840\ cm^{-1}$ band intensity and the increase in the $825\ cm^{-1}$ band intensity are detected on reducing the VDF content.

Such a treatment is now extended to the modes in a wider frequency region. By investigating the eigenvectors and potential energy distributions calculated for a series of model polymers, the vibrational modes can be classified into four types: (1) modes covering the VDF segments; (2) modes intrinsic to the TFE segments; (3) modes localized at the VDF–TFE boundary; and (4)

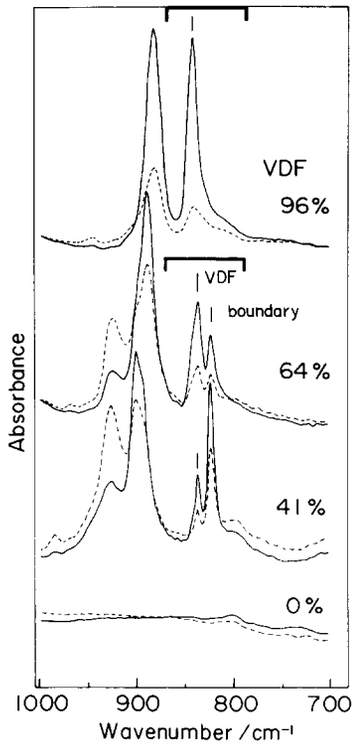

Figure 5 VDF content dependence of the observed polarized i.r. spectra of the VDF–TFE copolymers in the $700–1000\ cm^{-1}$ region. Electric vector of the incident i.r. beam (—) perpendicular and (– – –) parallel to the orientation axis

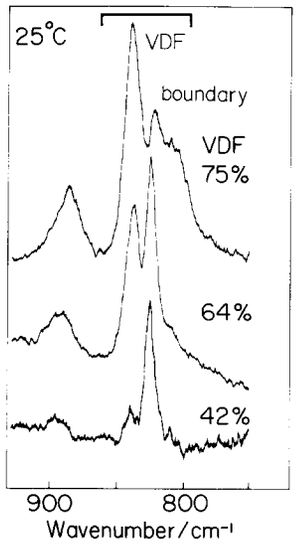

Figure 6 VDF content dependence of the observed Raman spectra of the VDF–TFE copolymers in the $700–1000\ cm^{-1}$ region

modes spreading over the whole chain. Modes (1) and (2) correspond approximately to those characteristic of homopolymers. Therefore they are expected to follow the frequency–dispersion curves calculated for homopolymers. Modes (3) and (4) are unique for a copolymer system. The intensity of mode (3) will be greatest for copolymers with an intermediate VDF content where the relative population of the boundary part in the copolymer chain is maximal. As illustrated in *Figure 3*, the phase angle between the adjacent VDF monomeric units can be estimated from the eigenvectors of each vibrational mode. *Figure 7* shows the curves obtained for the frequency–phase angle relation. The solid and broken lines denote the modes localizing on the VDF and TFE segments, respectively, which are coincident with the dispersion curves of PVDF and PTFE homopolymers[11,15,16]. The boundary modes appear in the vicinity of the frequencies at 825 and 921 cm^{-1} (shaded regions). *Figure 8* shows the frequency distribution calculated from the dispersion curve in *Figure 7*. The copolymer system has no translational symmetry along the chain axis and so no selection rule is applicable for the spectroscopically active modes. In other words, the frequency distribution function is useful to predict the

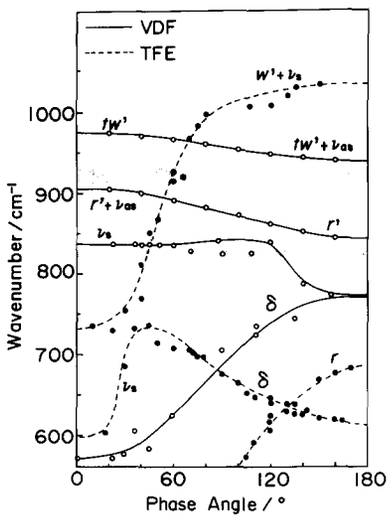

Figure 7 Frequency–dispersion curves constructed using the results of the normal-mode calculations for the VDF–TFE copolymer models. The phase angle is between the adjacent CF_2 oscillators. Solid curves represent the modes mainly contributed by the VDF segments. Broken curves represent the modes mainly contributed by the TFE segments. The shaded regions represent the modes localized at the VDF–TFE boundary region: w, wagging; tw, twisting; r, rocking; ν_s, symmetric stretching; ν_{as}, antisymmetric stretching; δ, bending mode of the CF_2 groups (t', w' and r' indicate some contribution of t, w and r to ν_s or ν_{as})

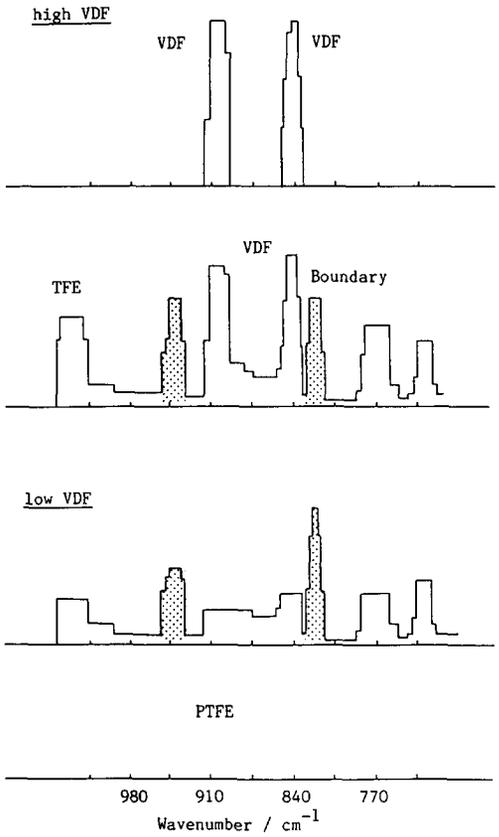

Figure 9 VDF content dependence of the frequency distribution functions speculated from *Figures 4* and *8*

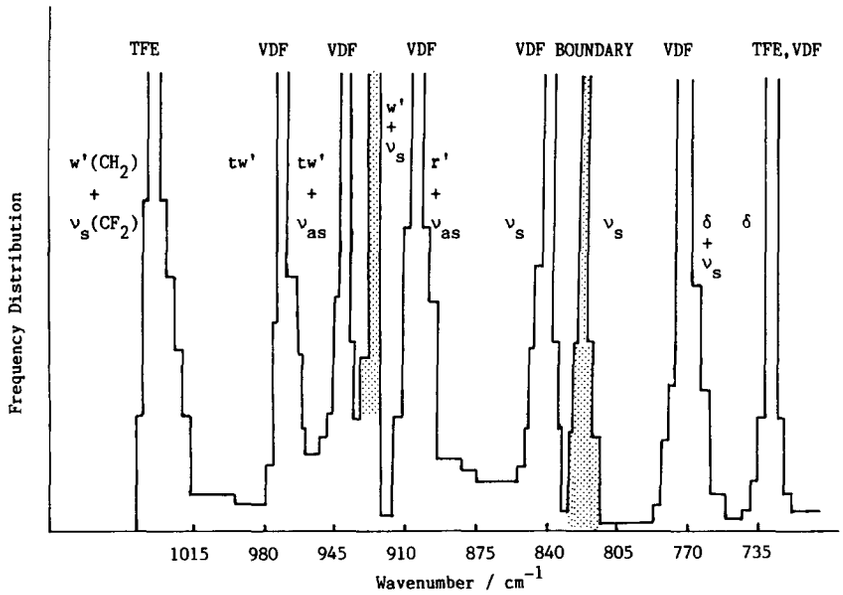

Figure 8 Frequency distribution function estimated from the frequency–dispersion curves in *Figure 7*

spectral change depending on the VDF content, as illustrated in *Figure 9*, where the frequency distribution curves are speculated from *Figures 4* and *8*. For copolymers with high VDF content, the peaks due to TFE and boundary parts are negligibly low and the two peaks intrinsic to the PVDF homopolymer will appear. As the VDF content is reduced, these VDF bands decrease in intensity and the bands originating from the boundary and TFE sequences increase gradually. In the other limiting case of PTFE, no band peaks appear in this frequency region because of the lack of optically active vibrational modes. Such a speculation described here is found to correspond well to the actually observed spectral change, as shown in *Figures 5* and *6*. We can confirm the band assignments made in our previous paper in this way[1]; that is, the 840 and 880 cm^{-1} bands are assigned to the modes intrinsic to the VDF *trans* sequences and the 825 and 925 cm^{-1} bands are assigned to the boundary modes.

In this paper we have interpreted the i.r. and Raman spectral changes measured at room temperature for a series of VDF–TFE copolymers by carrying out the normal-modes calculation based on simple model polymers. In the actual system, however, the VDF and TFE monomers are arranged in a statistical fashion along the chain axis. Strictly speaking, therefore, the models employed here should be modified into those with a statistical distribution of monomeric units. However, the results obtained may not be that different from those obtained here. We must also consider the effect of intermolecular interactions on the vibrational spectra, in particular on the low frequency lattice vibrational modes[5,6]. In order to analyse the spectral change caused by the *trans–gauche* conformational transition, the normal-mode frequency calculation must be carried out taking into account such a conformational change. This type of calculation is currently being carried out.

ACKNOWLEDGEMENT

The authors thank Daikin Kogyo Co. Ltd, Japan, for supplying the samples of VDF–TFE copolymers.

REFERENCES

1 Tashiro, K., Kaito, H. and Kobayashi, M. *Polymer* 1992, **33**, 2915
2 Tashiro, K., Takano, K., Kobayashi, M., Chatani, Y. and Tadokoro, H. *Polym. Commun.* 1981, **22**, 1312
3 Tashiro, K., Takano, K., Kobayashi, M., Chatani, Y. and Tadokoro, H. *Polymer* 1984, **25**, 195
4 Tashiro, K., Takano, K., Kobayashi, M., Chatani, Y. and Tadokoro, H. *Ferroelectrics* 1984, **57**, 297
5 Tashiro, K. and Kobayashi, M. *Polymer* 1988, **29**, 426
6 Tashiro, K., Itoh, Y., Nishimura, S. and Kobayashi, M. *Polymer* 1991, **32**, 1017
7 Renmo, C. and Minghui, H. *Japan-China Bilateral Symp. Polym. Sci. Technol.* 1981, 183
8 Bunn, C. W. and Howells, E. R. *Nature* 1954, **174**, 549
9 De Santis, P., Giglio, P. E., Liquori, A. M. and Ripamonti, A. *J. Polym. Sci. A* 1963, **1**, 1383
10 Tadokoro, H. 'Structure of Crystalline Polymers', Wiley-Interscience, New York, 1979
11 Kobayashi, M., Tashiro, K. and Tadokoro, H. *Macromolecules* 1975, **8**, 158
12 Tashiro, K., Kobayashi, M. and Tadokoro, H. *Macromolecules* 1981, **14**, 1757
13 Tashiro, K., Itoh, Y., Kobayashi, M. and Tadokoro, H. *Macromolecules* 1985, **18**, 2600
14 Zerbi, G. *Pure Appl. Chem.* 1971, **26**, 499
15 Zerbi, G. and Sacchi, M. *Macromolecules* 1973, **6**, 692
16 Masetti, G., Cabassi, F., Morelli, G. and Zerbi, G. *Macromolecules* 1973, **6**, 700